archives
of thermodynamics
Vol. **41**(2020), No. 3, 223–254
DOI: 10.24425/ather.2020.134578

The rectangular two-phase closed thermosyphon: A case study of two-phase internal flow patterns behaviour for heat performance

TEERAPAT CHOMPOOKHAM[a]
SURACHET SICHAMNAN[a]
NIPON BHUWAKIETKUMJOHN[b]
THANYA PARAMETTHANUWAT[b*]

[a] Heat-Pipe and Thermal Tools Design Research Unit (HTDR), Department of Mechanical Engineering, Faculty of Engineering, Mahasarakham University, Thailand

[b] Heat Pipe and Nanofluid Technology Research Unit, Faculty of Industrial Technology and Management, King Mongkut's University of Technology North Bangkok, Bangkok, Thailand

Abstract This research explored different types of two-phase flow patterns that influenced heat transfer rate by assessing rectangular two-phase closed thermosyphon (RTPCT) made from glass with the sides of equal length of 25.2 mm, aspect ratio 5 and 20, evaporation temperature of 50, 70, and 90 °C, working substance addition rate of 50% by volume of evaporator, and water inlet temperature at condensation of 20 °C. Upon testing with aspect ratios 5, three flow patterns emerged which were: bubble flow, slug flow and churn flow respectively. As per the aspect ratio 20, four flow patterns were discovered which were: bubble flow, slug flow, churn flow and annular flow, respectively. Aspect ratio 5 pertains characteristic which resulted in a shorter evaporation rate of the RTPCT than that of the aspect ratio 20, thus, a shorter flow distance from the evaporator section to heat releaser was observed. Therefore, flow patterns at aspect ratio 5 exhibited a faster flow velocity than that of the aspect ratio 20. Furthermore, changes of flow pattern to the one that is important for heat transfer rate can be easily achieved. Churn flow was the most important type of the flow for

*Corresponding Author. Email: thanya.p@fitm.kmutnb.ac.th

heat transfer, followed by slug flow. Moreover, with aspect ratio 20, annular flow was the most important flow for the heat transfer, followed by churn flow, respectively. Throughout the test, average heat flux as obtained from the aspect ratio 5 were 1.51 and 0.74 kW/m^2 which were higher than those of the aspect ratio 20. The highest heat flux at the operating temperature of the evaporator section was 90 °C, which was equivalent to 2.60 and 1.52 kW/m^2, respectively.

Keywords: Internal flow; Flow pattern; Rectangular two-phase closed thermosyphon

1 Introduction

Two-phase closed thermosyphon (TPCT), shown in Fig. 1, is a type of heat pipe with no porous materials as a component. TPCT consists of 3 parts, evaporator, heat protector, and condenser and is produced from steel, stainless steel, and copper pipes. Both ends of TPCT are welded by the same materials that are used to make the pipe. Upon receiving of heat from a heat source, TPCT's evaporator will pass through the heat *via* inner wall of the pipe to the working substance until the substance's temperature is higher than its saturated temperature [1–3].

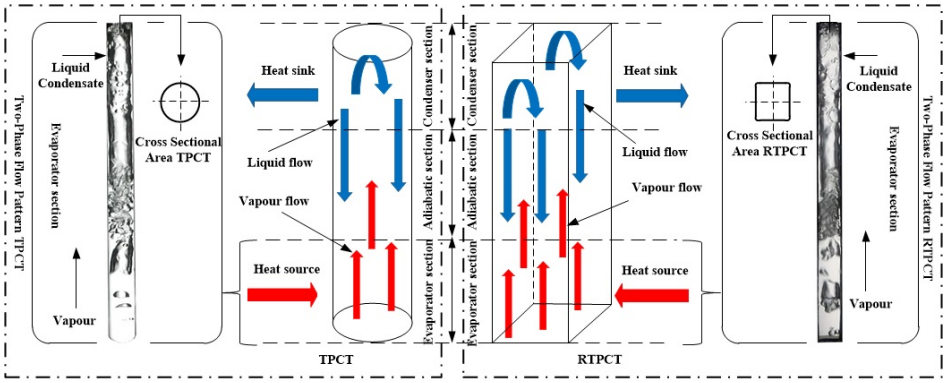

Figure 1: Characteristics and flow patterns of TPCT and RTPCT.

Whilst the evaporator's temperature increases, viscosity and density of the working substance decreases. The boiling of working substances transforms its state from liquid to gas that leads to bubble flow pattern which accumulate energy as velocity and pressure [4]. Bubble flow will be initiated as speed and pressure increased. Thus, the bubbles will be merged or mixed with other bubbles which created a bigger vapor lumps. The size of such

vapor lumps increases as a longer distance of movement is covered. This type of flow resembles a bullet shape flow, thus, it is also called a slug flow. After a period of flow, slug flow movement will be distorted which lead to asymmetric flow due to the increased speed and pressure. This will eventually lead to a flow pattern known as the churn flow [5]. When the flow pattern moved at the highest speed and pressure, gaseous state will be detected at the center of the pipe whereas the working substance, as liquid state, flows on the side of the pipe back from the condenser towards the evaporator. This flow pattern is known as annular flow [6] as shown in Figs. 1 and 4b. The two-phase flow pattern, liquid and gas phases, in the TPCT moves from the evaporator through the adiabatic to the condenser section respectively which liquefied gaseous working substance into liquid form. Two-phase closed thermosyphon uses evaporation and condensation mechanisms of the working substance to transfer the heat. Liquid working substance from the condensation unit is drawn back to the evaporator again by the gravity. Such cycle of work will continue continuously [7,8]. The two-phase closed thermosyphon attracts inexpensive construction costs, and exhibits a simple structure that requires no external energy to operate. TPCT has very little heat resistance, thus, works highly efficiently even at little differences in temperature between the heat source and the heat receptor. TPCT requires relatively low maintenance costs. The industrial sector, therefore, applies TPCT as a cooling device, particularly when the heat reuse is required. These industries are electronic components, cooling turbine blades, heat system, and solar power etc. On the contrary, TPCT may encounter two main problems: heat transfer – due to the counter flow behavior between the gaseous and liquid working substance at the heat and condensation component which directly affects the heat transfer. Moreover TPCT is mostly manufactured from a round tube or a cylindrical cross-sectional tube which influences the installation and application to work areas that require cooling or heat exchange [7]. Therefore, there have been attempts to study the two-phase closed thermosyphon (TPCT) including a heat pipe (HP) with a cross-sectional surface area (or cylindrical cross-sectional surface area) other than the circular cross-sectional one in order to reduce the above mentioned problems. Previous research revealed that circular two-phase closed thermosyphon (CTPCT) which evolved to become the flat two-phase closed thermosyphon resulted in volume reduction of the pipe. Thus, the cross-sectional surface area directly affects the addition ratio working substance (when addition ratio is the same). As a result, working substance inside the pipe, upon being heated at the evaporator,

boils and quickly changes from liquid into vapor. Therefore, heat transfer capability is higher than CTPCT [9, 10]. According to the shape adjustment, CTPCT and flat-FTPCT alters addition rate of working substance, aspect ratio, and different heat feeding rate at evaporator. The test utilized water as a working substance which suggested that flat-FTPCT required a higher evaporation temperature than that of CTPCT. The highest heat fed to the evaporator directly affected the heat flux. For each test, increased adding rate of the working substance, aspect ratio, and heat flux also increased the aspect ratio and the heat feeding rate at the evaporator section [11]. In case of the study of performance of a small heat pipe that has a cross-sectional adjusted for cooling of notebook personal computer, three type of heat pipe were used in this test consisting of circular woven wire wick, composite wick and central wick. Upon pressing, the cross-sectional surface area is reduced by 30% (circular cross-sectional surface area) for which the composite wick appeared to be the most effective one. As a result, the heat generated by CP notebook computers was reduced by 10% [12]. In the study on application of a small heat pipe with a polygonal cross-sectional modification for cooling personal computer's CPU a small heat pipe with triangular and square cross-sectional surfaces were used. The length of the evaporator, heat protector, and condensation were 10, 15, and 25 mm, respectively. The results showed that, small heat pipes with triangular cross-sectional provided higher heat resistance property than the pipe with a square cross-sectional surface [13]. There were studies concerning the effects of non-porous heat pipe with adjusted cross-sectional surface area on working substance addition ratio that affects performance of flat-panel solar energy collectors. The heat pipe used in the studies consisted of 3 cross-sectional surface areas, circular, oval and semi-circle. The addition rate of the working substances (water) used in the tests were 10%, 20%, and 30%. The results showed that, at lower addition rates, flat-panel solar energy collectors with the oval cross-section surface heat pipe performed better than that of the circular cross-sectional surface pipe. Working substance addition ratio 10% was suitable for pipe with the oval cross-sectional surface area while the heat pipe with circular cross-sectional surface area performed better than the addition rate of 20%. At the addition ratio 20%, the heat pipe with semi-circle cross-sectional surface area performed worse than other types of the pipe [14]. Upon considering the boiling and condensation of working substances, and the thermal efficiency of the flat two-phase thermosyphon with the grooved evaporator, water performed better than ethanol as the working substance. Furthermore, the grooved evaporator in-

creases the surface areas for boiling which results in a much better efficiency [15]. Rectangular two-phase closed thermosyphon was also tested for its efficiency by using water, silver nanoparticles (NP) suspension water, and silver nanoparticles suspension water with oleic acid surfactant (NP+OA) (as surface tension reductant) as working substances. Heat at the evaporator was 20, 40, 60, 80, and 100% produced by a 2000 W heater. Results suggested that the heat transfer capacity increases according to the heat applied to the evaporator increases. In addition, the use of silver nanoparticles suspended water with NP+OA as the working substance provided the best heat transfer [7]. Studies of two-phase closed thermosyphon with different cross-sectional surface areas help to determine its advantages, benefits and various applications. This research focused on the study of the rectangular two-phase closed thermosyphon with the contact area for receiving and releasing heat, at respective heat source and the heat receptor, that perform better than that of the circular two-phase closed thermosyphon as shown in Fig. 8. This helps to eliminate the heat resistance between the heat source and the external surface of the evaporator (Z_1) as well as eliminating heat resistance between the external surface of the evaporator and heat releaser (Z_9), respectively. As a result, RTPCT has total heat resistance (Z_{total}) less than that of TPCT, as shown in Fig. 3 [7]. Adjusted cross-sectional surface area provides appropriate site that helps to reduce the friction caused by the two-phase flow. Furthermore, having a thin liquid film produced by condensation at the condenser (subject to density as well) also helps the bubbles and vapor to move quicker from the evaporator to the condenser. This is also related to a higher heat transfer coefficient as well [9].

Two-phase flow pattern consisting of liquid and gaseous states is the fundamental factor of the heat transfer efficiency characterized by the two-phase closed thermosyphon and heat pipe. Each flow pattern provides different heat transfer capabilities. The nature of each flow pattern is characterized by related variables such as cross-sectional surface area, shape of the pipes used in the production of TPCT and HP, surface areas for heat receptor and releaser, length of the pipe, test angle, working substance addition rate, temperatures at evaporator and condenser, working substance type, pipe inner diameter, wetted perimeter, and hydraulic radius size. These variables are all related to the formation of two state flow patterns and the total heat transfer [16, 17]. Flow patterns and their behaviors have been widely studied including those concerning heat transfer characterized by the flow of working substance in the two-phase loop thermosyphon. The working substance used was R134a with the adjusted evaporation cham-

ber. According to the test, and at the height of the evaporation channel, the bubble flow was amalgamated with the slug flow. At high heat flux, slug and churn flows were observed. Furthermore, it was evidenced that the flow and thermal instability increased as the height of the evaporating channel decreased whereas the heat transfer coefficient was increased when the height of the evaporating channel and heat flux increased [18]. According to a study on the circular two-phase closed thermosiphon with the pipe diameter of 11.1 mm that used R-123 as a working substance, addition ratio 80% of the total volume, aspect ratio 30, 10, and 5, revealed that, at the aspect ratio 30 at the test angle of 90° from horizontal plane, the maximum heat flux was equal to 20.7 kW/m^2. In the upper part of the evaporator, annular flow (AF) and churn flow (CF) were discovered whereas at the center and bottom parts, slug flow (SF) and bubble flow (BF) were discovered, respectively. Most of the flow patterns found at a 90° test angle were annular and churn flows mixed with the slug flow. Upon adjusting the test angle to 30°from the horizontal plane, maximum heat flux level discovered was 24.6 kW/m^2. At the bottom of the evaporator, bubble flow was reported whilst the middle part of the evaporator slug flow with high, extended wave of liquid were found. On the other hand, the upper part of the evaporator exhibited the flow that were separated in layers. Bubble and slug flows were the main flows found at the test angles of 30°, while at the test angle of 5°. The maximum heat flux level was 16.7 kW/m^2. At the bottom and center of the evaporator, slug flow with liquid wave reported. In the upper part of the evaporator, slug flow and liquid waves that were emitted from the lower part were found. The main flow patterns reported were bubble flow and slug flow together with slightly expanded liquid wave. At the aspect ratio 30 and 10, the flow's characteristics and behavior were mostly similar. At the aspect of 5, with the test angle of 90°, 30°, and 5°, the maximum heat fluxes were 78.6, 92.4, and 53.9 kW/m^2, respectively. Bubble flow (and bubble merging) was the main flow pattern found at the test angle of 5° from the horizontal line [4]. As per the flow patterns tested with circular two-phase closed thermosyphon, the working substances used were water, ethanol, and HFE-7000. The internal diameter of the TPCT was 8 mm with the evaporator length of 100 mm, the heat protector length of 180 mm and, and the condenser length of 200 mm. Tests that used water and ethanol as the working substance were conducted with the heat flux 7.5 and 7.0 kW/m^2, respectively. The geyser boiling pattern was found to have low vapor pressure and high vapor production rate. Slug flow and plug flow were reported at 5.5 and 5.7 kW/m^2 of heat fluxes, respectively. High va-

por pressure and low vapor production rate were reported when tested with 17.0 kW/m^2 heat flux. The churn flow was initiated at high vapor pressure, and high vapor production rate while the surface tension was relatively low when ethanol was used as the working substances. When HFE-7000 was used as a working substance at the heat flux of 7.8–21.5 kW/m^2 pool boiling at the evaporator was observed. Vapor bubbles production rate was high but the bubbles were smaller than the test that used water as working substance [19, 20]. All tests using HFE-7000 as a working substance resulted in less condensed liquid that flowed back to the evaporator. This was a result of the low surface tension when compared to ethanol water [20]. The study of the two-phase flow pattern in the circular two-phase closed thermosyphon as a small heat exchanger. Tested TPCT is made of glass tubes with; inner diameter of 16 mm, total length of 290 mm, acetone as working substances, 80% addition rate, test angle of 0, 5, 10, 15, 20, 30, 60, and 80° and the provided heat flux ranged 0 to 32 kW/m^2. As per the results, vapor plugs were found at all angles of the test with a heat flux below 14 kW/m^2 whereas a annular flow was found at a heat flux between 14 and 32 kW/m^2. The wave dispersed faster as the heat flux increased [21]. As per the test that used glass circular two-phase closed thermosyphon with graphene-acetone nanofluid at the concentration of 0.05%, 0.07%, and 0.09% as the working substance, upon applying the heat at the evaporator of 1 W, discontinuous bubble flow was initiated. Upon increasing the heat to 20 W, the bubble flow was observed with higher number of bubbles. At 30 W heat, churn flow pattern was found. When the heat was increased to 40 and 50 W, the flow pattern changed from churn flow to annular flow. In addition, heat resistance was reduced to a maximum of 70.3% and the heat transfer coefficient of the evaporator was increased to 61.25% (when graphene-acetone nanofluid at 0.09% concentration was used). Annular flow provided higher heat transfer coefficient compared to other flow patterns [22]. Annular flow and churn flow were the type of flow that affected heat transfer [4, 20, 22]. According to the test of a glass circular two-phase closed thermosyphon with; internal diameter of 13 mm, total length of the TPCT of 930 mm, Freon 113 as a working substance, test angles of 90°, 80°, 70°, 60°, 55°, 45°, 35°, 20°, and 5° from horizontal plane, annular flow was observed along the vertical or at a position near such vertical. In case of the flows that were separated in layers, dry out occurred at the top surface of the pipe. Dry out is an efficiency limitation on the inclined TPCT. Dry out is not a character of the annular flow. Heat transfer rate of the annular flow is very different from the other flow types that has dry out [23]. Ac-

cording to a study on the flow of working substance and factors affecting the heat transfer mechanism of U-shaped thermosyphon, three flow patterns were found, slug flow, annular flow, and oscillation of a liquid mass. The slug flow and annular flow, compared to the oscillation of liquid mass, carries a better heat transfer. Main factors affecting the efficiency of the U-shaped thermosyphon are the substance addition rate and the working substance. U-shaped thermosyphon which uses R134a as a working substance has a better performance than the one that uses R113 as a working substance. This was due to R134a's lower boiling point than that of R113 [24]. There was a study on the flow of ethanol mixed with nanoparticle of silver powder, and ethanol as the working substances. The pipe used in this study was circular oscillating heat pipe equipped with a reversing valve made of glass pipes with a circular cross-sectional surface area with the internal diameter of 2.4 mm. Results revealed that at; evaporator temperature of 125 °C, test angle of 90°, the highest heat flux reported was 2.04 and 1.31 kW/m^2 when used ethanol mixed with nanoparticle of silver powder, and ethanol as working substances, respectively. The main flow patterns found in both test cases were dispersed bubble flow which showed small bubbles in the lower part of the evaporator. The bubble extended to the bottom of the evaporator before moving to the condensation section [25]. Flow patterns can also be used to signify the system stability. Flow instabilities in a horizontal thermosyphon reboiler loop was studied which uses water as a process liquid and steam as a heat transfer. According to the result, the liquid flow rate was an important factor that led to system instability. Once the system was stabilized, the heat flux was higher than 20 kW/m^2. A stable system normally show heat flux between 11–20 kW/m^2. Flow pattern within the system affected the liquid flow rate as different flow patterns results in different speeds and properties. Most of the flow patterns were of basic flow patterns for which annular flow gave a high quality of heat flux and flow rate. The heat fluxes were reducing, in successive order, from annular flow, churn flow, slug flow, and bubble flow [26]. Two-phase closed thermosyphon that was equipped with glass tubes, and ethanol as a working substance showed a working cycle that started when the evaporator was being heated, the working fluid in the liquid state began to boil. Once generated, the steam passed through the adiabatic part to the condenser and condensed at the upper part of the TPCT before flowing back to the evaporator as a liquid substance again. At the same time, the vaporization from the evaporator started to condense again [22, 27, 28]. Two-phase flow patterns within the circular oscillating

heat pipe made of glass with a diameter of 2 mm was also studied. The test position was horizontal with the length of evaporator, adiabatic, and condenser at 50 mm per each section. Water and ethanol were used as working substances and the heat supplied to the evaporators was at 80, 90, 100, and 110 °C. Results showed that the flow was divided into two main parts including oscillation of the slug flow, and the one that remained immobile. The cooling efficiency was improved when 10 turns of closed-loop oscillating heat pipe which created small vapor bubbles. Oscillation flow was maintained for quite a long time at 50% addition rate with the lowest heat resistance reported with water and ethanol as the working substances. The heat supplied to the evaporator was at 100 °C which showed the lowest heat resistance when using water as the working substance [29]. A study on the flow pattern and heat transfer of the circular cross-sectional surface area pipes with inner diameter of 4.26 mm and 2.01 mm, 6 flow patterns were reported consisting of dispersed bubble flow, bubble flow, slug flow, churn flow, annular flow, and mist flow respectively. Changes of internal diameter from 4.26 to 2.01 mm affected the flow pattern which was changed from the slug flow to churn flow and annular flow. Heat transfer was facilitated by two-phase flow in the pipe for which the heat transfer coefficient was a function of the heat flux and the system pressure but was not subject to quality of the vapor and mass of the flux. According to the test with a pipe with an internal diameter of 4.26 mm, the vapor quality was less than 40–50% whilst the heat transfer coefficient increased in response to the heat flow rate and the system pressure but was not affected by the vapor quality. Thus, within this range, the dominant vapor was nucleate boiling. For pipes with an inner diameter of 2.01 mm, the vapor quality of less than 20–30% was discovered [30]. Fluctuated heat transfer within the two-phase closed thermosyphons which used water, ethanol, and acetone as working substance and as observed from the test, changes in heat transfer is strongly related to vapor bubble behavior and physical properties. The low working pressure led to instability of the heat transfer. In the two-phase closed systems, temperature variations and the heat transfer coefficient of the evaporator were mainly caused by the behavior of the bubbles [31].

According to the study of flow patterns and behavior within TPCT and HP, the cross-sectional surface area or different shape of the pipe were important variables that affected the boiling of the working substance in the evaporator, the formation of the flow pattern, the proportion of the flow pattern occurrence, the behavior of the flow patterns, and the speed of each flow type. All of these factors were related to the heat transfer efficiency

of the two-phase closed thermosyphon. Thus, rectangular two-phase closed thermosyphon (RTPCT) is difference from TPCT as previously described. Previous studies on TPCT lacked information regarding RTPCT which gave rise to the study concept of this research. Benefits of the study will include understanding on the nature of the cross-sectional surface area or the shape of the thermosyphon with rectangle cross-sectional surface area. Moreover, evaporator temperature and the aspect ratios that influence the two-phase flow behavior and the heat transfer characteristics of RTPCT, together with the data obtained from this study, can also be used to describe the characteristics of the heat transfer. This also provide the basic information for RTPCT designing that would provide a higher efficiency in the future.

2 Theoretical consideration

2.1 Different cross-sectional geometry characteristics

Rectangular two-phase closed thermosyphon is characterized by the external contact of the circular two-phase closed thermosyphon, which include the cross-sectional surface area, wetted perimeter, and hydraulic radius. In the case of different geometry cross-sectional thermosyphon (DGCST) this is showed as shown in Fig. 2. Upon considering the heat transfer capacity, this would be depending on heat resistance of the TPCT/RTPCT that formed in the evaporator, heat protector, condenser [10, 32].

The cross-sectional surface area can be calculated by

$$A = \frac{\pi Y^2}{4} + (XY). \tag{1}$$

The wetted perimeter can be calculated by

$$W_{perimeter} = \pi Y + 2X \ . \tag{2}$$

The hydraulic radius can be obtained from the equation

$$R_h = \frac{(\pi/4)Y^2 + (XY)}{\pi Y + 2X} \tag{3}$$

is meaning $4R_h = D_i$. The aspect ratio can be obtained from the relation

$$\frac{L_e}{D_i} = \frac{L_e}{4R_h}\,, \tag{4}$$

where L_e denotes the evaporator length. The shape characteristics of RTPCT can be found from Eqs. (1)–(4) which have been reported by [10, 32].

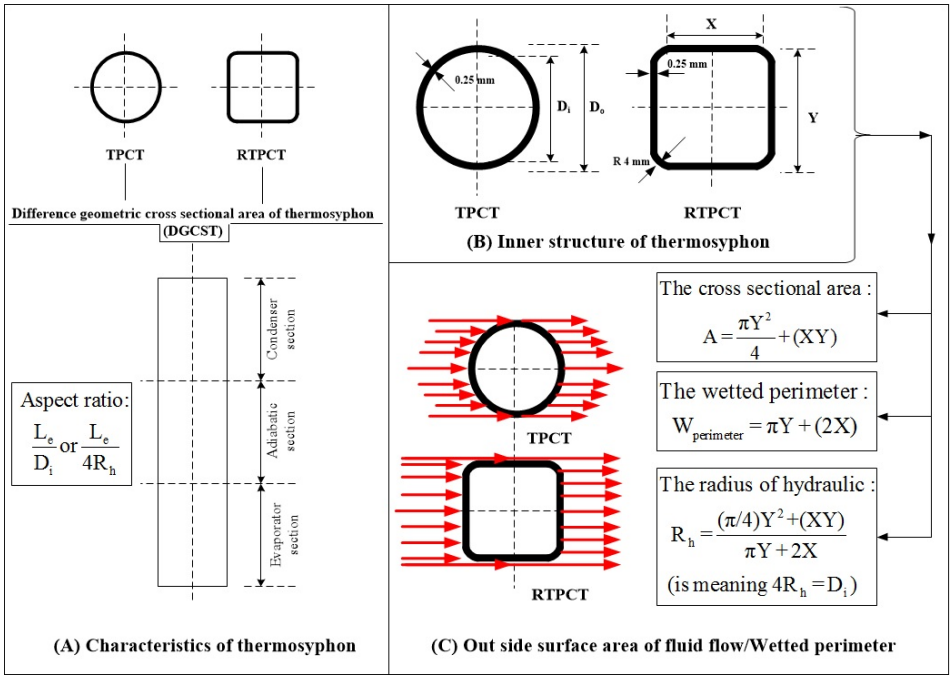

Figure 2: The shape and characteristics of TPCT and RTPCT.

2.2 Heat transfer characteristics

The heat transfer efficiency of TPCT ($Q_{Theoretical}$) can be calculated from the proportion of temperature difference between evaporator and condenser (ΔT) whereas total heat resistance (Z_{Total}) can be obtained from Eqs. (5) and (6) [2]

$$Q_{Theoretical} = \frac{\Delta T}{Z_{Total}} \tag{5}$$

(ΔT) can be calculated by

$$\Delta T = \frac{(T_{h,\,in} - T_{c,\,out}) - (T_{h,\,out} - T_{c,\,in})}{\ln \dfrac{(T_{h,\,in} - T_{c,\,out})}{(T_{h,\,out} - T_{c,\,in})}} \,. \tag{6}$$

Z_{Total} is the total heat resistance shown in the thermal model by Engineering Sciences Data Unit Item No. 80023, ESDU 81038 [33] which consists of the heat resistance from 3 parts, as shown in Fig. 3, as follows:

- The first part is the external resistance, Z_1 and Z_9 that represent the resistance from the external convection of the pipe.
- The second part is the resistance from material property, Z_2 and Z_8 represent the resistance from the thermal conductivity of the material.

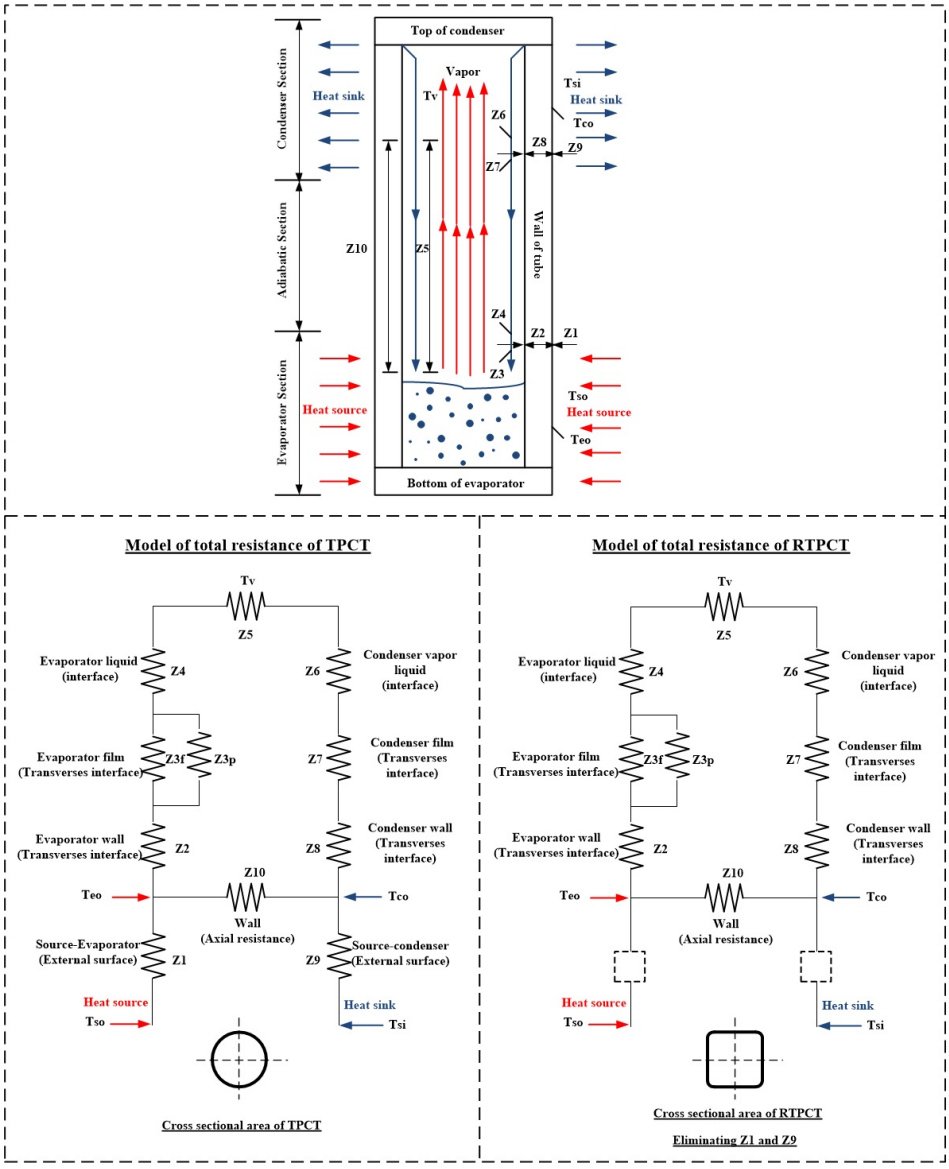

Figure 3: The total heat resistance model of TPCT and RTPCT [7].

- The third part is the internal resistance Z_3, Z_4, Z_5, Z_6, Z_7, and Z_{10} that represent the internal resistance due to the working fluid of pool and film boiling.

As surface area of the RTPCT is different from that of TPCT as shown in Fig. 8, external heat resistance Z_1 and Z_9 at the evaporator and the condenser section can be eliminated. The total heat resistance model of TPCT and RTPCT are shown in Fig. 3.

3 Test equipment installation and analysis

3.1 Test set installation and testing

Figure 4 shows the installation diagram of the test set and the testing. Rectangular two-phase closed thermosyphon is set by removing air using a vacuum pump, to create a vacuum environment, before an addition of a working substance as shown in Fig. 4a. The variables used in the test consisted of: RTPCT with length of X and Y equal of 25.2 mm, aspect ratio 5 and 20, water as a working substance, addition rate of working substance at 50% of volume of evaporator, inlet temperature at condenser 20 °C, mass flow rate of inlet condenser at 0.25 l/min, test angle of 90° to the horizon plane, and evaporator temperatures of 50, 70, and 90 °C, as show in Tab. 1.

Table 1: Controlled and variable parameters.

Independent variable	– evaporator temperature at 50, 70, and 90 °C, (T_e) – aspect ratios equal to 5 and 20. (AR)
Dependent variables	– effect of aspect ratio and the evaporator temperature to the flow patterns two-phase closed rectangular cross section area thermosyphon. – effect of aspect ratio and the evaporator temperature to heat transfer rate and heat flux two-phase closed rectangular cross section area thermosyphon.
Control variables	– distance of sides X and Y were 25.2 mm (X, Y) – working fluids; de-ionized water – inclination angle equal 90° (AI) – temperature of water in the condenser section equal 20 °C (T_c) – mass flow rate of feed water equal to 0.25 l/min – filling ratio equal to 50% with respect to evaporator section

As for the test, as shown in Fig. 4b, hot water from the hot water bath was drawn into the evaporator. Evaporator temperature was controlled by a temperature control unit. Cold water flowed from the cold water basin

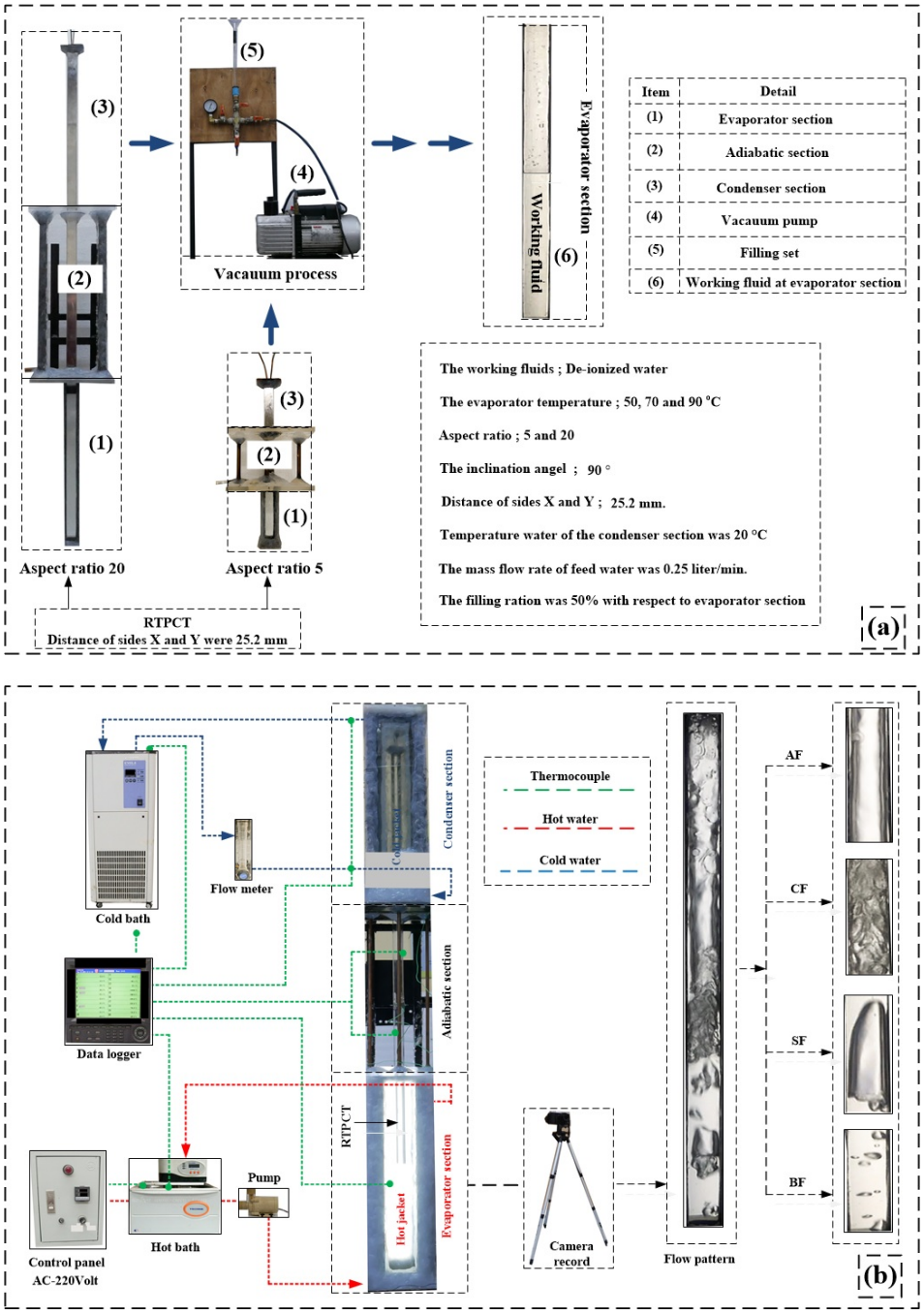

Figure 4: Test installation diagram and testing.

through the mass flow meter into the condensation section. When the test system reached equilibrium, recorded a video at the evaporator section. At the same time, measured the temperature at 9 different parts using the K-type thermocouple with ±1.5 °C deviation. The temperatures were recorded with data logger (Yokogawa DX200) with 1 °C deviation. The flow meter used was Disco-BBBW1B98 with ±5% accuracy. Temperature measurement points consisting of: hot water at evaporator, hot water temperature at hot water tub, temperature control unit, data logger, 2 points at adiabatic section, environment temperature, inlet water to condenser, outlet water from condenser, and cold water basin. Outlet water's temperature at the condenser can be used to calculate heat transfer rates, which can be found from Eq. (1).

3.2 Analysis of heat transfer rates and flow patterns

The heat transfer in RTPCT begins when the working substance contained within the evaporator is heated through the pipe wall. The working substance is changed from liquid to a vaporous form, passing through the heat protector before reaching the condenser which is lower in temperature. The heat is transferred to heat receptor substance, which in this case uses water. The heat transfer can be calculated from [34]

$$Q = \dot{m} C_p (T_{co} - T_{ci}) \,, \tag{7}$$

when Q is the heat transfer rate, $\dot{m}$ is the mass flow rate of water, C_p is the specific heat capacity of the water, T_{co} is the water outlet temperature of the condensation section is the water inlet temperature of the condenser.

Mass flow rate can be obtained from

$$\dot{m} = \rho v A \,, \tag{8}$$

when ρ is the density of water, v is the speed of water, A is the cross-sectional surface area of the water flow.

Heat flux can be obtained from

$$q = \frac{Q}{A_c} = \frac{Q}{\pi D_o L_c N} \,, \tag{9}$$

where D_o is the pipe's outside diameter, A_c is the external surface area of the condenser of the pipe, L_c is the length of the condenser of the pipe, N is the number of RTPCT or TPCT of the condenser.

Flow pattern within RTPCT is continuously recorded as video frames for which the recorded information is presented as projecting images or still images at a rate of 60 fps (frames per second). The percentage of the flow pattern, can be calculated from the area (width × length) of each flow pattern and the percentage of the flow pattern is based on an average of the 3 cycles that are recorded continuously with the video cameras.

The percentage of each flow occurrence can be calculated from the equation

$$(\%)\ \text{Each flow pattern} = \frac{\text{Number of grid for each flow pattern}}{\text{Total grid}} \times 100\,. \quad (10)$$

Number of grid refers to hypothetical grid number that helps estimate the length, position or work area of projected images or still images. The grid is a square with equal spacing of each box.

3.3 Uncertainty analysis

Measurements of uncertainty, the calculations are divided into two types. Type A is the uncertainty due to a random source that has been statistically evaluated which can be calculated from the following equation. When $\overline{x}$ denotes arithmetic mean and SD is standard deviation:

$$\overline{x} = \frac{x_1 + x_2 + x_3 + \ldots + x_n}{n_s}\,, \quad (11)$$

$$\text{SD} = \frac{\sqrt{(x_1 - \overline{x})^2 + (x_2 - \overline{x})^2 + (x_3 - \overline{x})^2 + \ldots + (x_n - \overline{x})^2}}{n_s - 1}\,, \quad (12)$$

$$u_{i,\,type\,A} = \frac{\text{SD}}{\sqrt{n_s}}\,, \quad (13)$$

where n is the number of measurements in the experiment.

Type B is the uncertainty due to system errors which can be calculated from the following equation:

$$u_{i,\,type\,B} = \frac{a}{\sqrt{3}}\,, \quad (14)$$

where a is the semi-range (or half-width) between the upper and lower limits.

Combined standard uncertainty, i.e., the sum of uncertainty types A and B can be calculated from the following equation:

$$u_c = \sqrt{(u_{i,\,type\,A})^2 + (u_{i,\,type\,B})^2 + \dots} \ . \tag{15}$$

Expanded uncertainty can be calculated from the following equation:

$$U = ku_c \ . \tag{16}$$

When $k = 2$ is correct, if the combined standard uncertainty in normally distributed results in the level of confidence of approximately 95% [35, 36].

For other coverage factors (normal distribution):

$k = 1$, for the confidence level of approximately 68%;

$k = 2.5$, for the confidence level of 99%;

$k = 3$ for the confidence level of 99.7%.

The results of uncertainty analysis of this study are displayed in Tab. 2.

Table 2: Uncertainty analysis result.

Type	Quantity source of uncertainty	Value of quantity	Confidence level (%)	Converge factor k	Standard uncertainty (u_i)	Sensitivity coefficient (c_i)	Uncertainty (u_i, c_i)	Combined uncertainty component	Expanded uncertainty (U)
A	Uncertainty of mean reading (°C)	–	95	2	0.00229	1	0.00229	0.53073	1.06146
B	Thermocouple type K (°C)	$-200-1,372$	95	2	0.86602	0.99817	0.86443		
B	Data logger (°C)	$-200-1,100$	95	2	0.57735	0.99846	0.57646		
B	Flow meter (kg/s)	0.167–0.3	95	2	0.02886	0.39975	0.01153		

4 Results and discussion

Flow pattern in RTPCT focused on the case study for which the aspect ratio and evaporator temperature affect the internal flow pattern of RTPCT.

4.1 Behavior of flow patterns within RTPCT

The flow behavior, as shown in Fig. 5, is based on the specific analysis of the flow patterns within the evaporator of the RTPCT. The process starting from the heat source that provides the heat to the evaporator's

pipe surface which gradually rise in temperature before the heat is passed through from the pipe wall to the working substance. When the working substance receives more heat accumulation, its viscosity and density decreases. As temperature inside the evaporator increases, differences in pipe surface temperature and temperature of the working substances become greater as well. The working substance (liquid state) starts to boil changes into vapor and forms bubbles. At the same time, fluid movement also occurs within the evaporator of the RTPCT [37, 38]. This results in small vapor bubble boiling that also present velocity and pressure energy. Such increase in velocity and pressure of the bubble flow pattern, combined with the in-

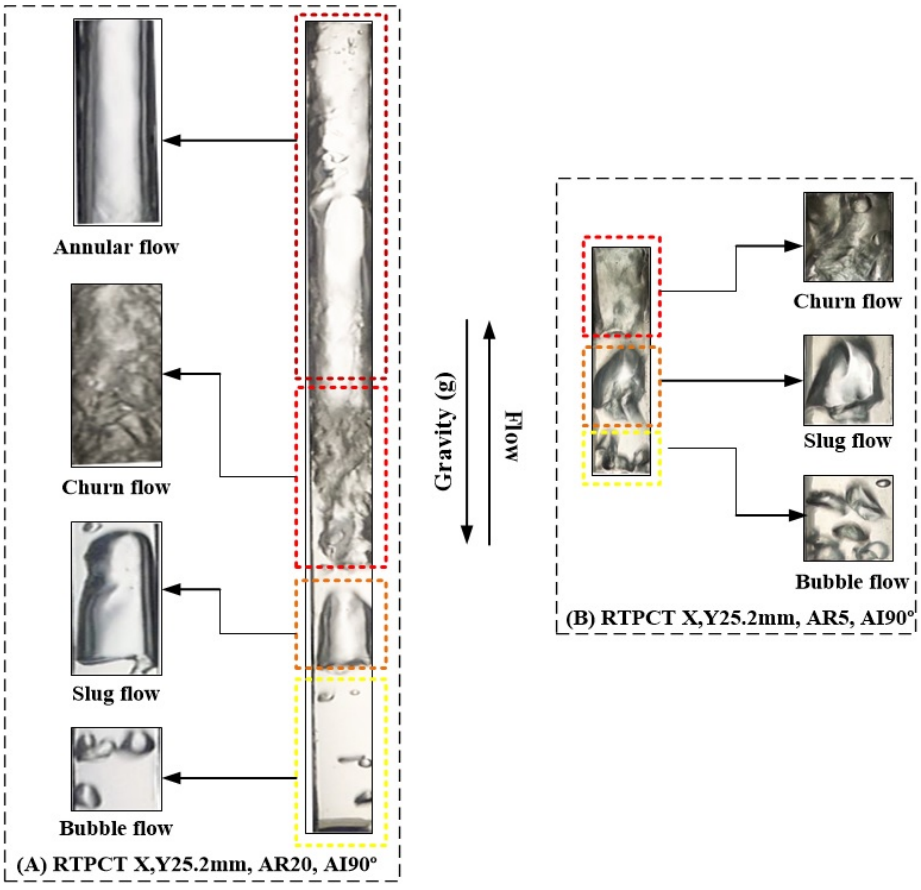

Figure 5: The two-phase flow pattern within RTPCT with the length of the X and Y of 25.2 millimeters, the test angle of 90°, for (A) with the aspect ratio of 20 and (B) with the aspect ratio of 5.

crease in the number of vapor bubbles, resulting in collision and merging of bubbles. Thus, the vapor bubble become larger in size which resemble a bullet which is also known as a slug flow [39]. With higher speed and pressure, bullet-like vapor bubbles begin to distort and break apart which leads to instability. In certain case, forepart of bullet bubbles collide with one another which change the flow pattern from slug to churn flow. At very high vapor velocity, an empty space in the middle of the pipe is formed for which gaseous substance will flow in the middle of the pipe while the liquid film substance stays on the pipe surface. This type of flow is called the annular flow [40]. The two-phase flow pattern as above described can be found in the test with RTPCT with the X and Y length of 25.2 mm, aspect ratio of 5 and 20, test angle of 90° against the horizontal plane as shown in Fig. 5. The behavior and the two-phase flow patterns inside the RTPCT will move upward to the condenser. When the working substance condenses and changes from vapor to liquid, the working substances becomes heavier and moves downward due to the earth gravity of the earth. Once the liquid working substance reaches the evaporator, it will be heated and the working cycle is repeated [38, 41].

4.2 Effects of the aspect ratio and evaporator temperature on the two-phase flow patterns

As per a study of the aspect ratio of 20, evaporation temperature of 50, 70, and 90 °C of RTPCT with the length of the X and Y sides of 25.2 mm, test angle of 90°, and water working substance, the results, as shown in Tab. 3(A), showed that at evaporation temperature 50 °C, the flow pattern was not discovered within RTPCT. At evaporator temperature of 50 °C, the heat from the heat source that was passed through the hot jacket and transfer heat to evaporator's pipe wall of RTCT and on to working substance was insufficient to overcome the molecular force between the working substance and the particles that make up the pipe's wall. Similarly, the evaporation temperature of 50 °C was insufficient to instigate the latent heat of vaporization in the working substance to boil. Thus, the two-phase flow was not found at this temperature. Upon increasing the temperature to 70 and 90 °C, 4 types of flow patterns were reported including: bubble flow (BF), slug flow (SF), churn flow (CF), and annular flow (AF), respectively. Increasing evaporation temperature resulting in lower viscosity and density of the liquid working substance, then the working substance will start to boil and evaporate. This gives rise to a two-phase flow pattern con-

Table 3: (A) Effects of evaporator temperature and aspect ratios on flow pattern and heat transfer when using RTPCT with the lengths of the X and Y of 25.2 mm, the aspect ratio 20, and the test angle of 90° (Ug is velocity of flow pattern, Lv is length of flow pattern).

The evaporator temperature (°C)																										
90 °C												70 °C												50 °C		
$Q = 77.65$ W $q = 1.52$ kW/m^2												$Q = 25.62$ W $q = 0.50$ kW/m^2												$Q = 10.81$ W $q = 0.21$ kW/m^2		
Annular flow			Churn flow			Slug flow			Bubble flow			Annular flow			Churn flow			Slug flow			Bubble flow			No flow patterns		
%	Ug (m/s)	Lv (m)	%	Ug (m/s)	Lv (m)	%	Ug (m/s)	Lv (m)	%	Ug (m/s)	Lv (m)	%	Ug (m/s)	Lv (m)	%	Ug (m/s)	Lv (m)	%	Ug (m/s)	Lv (m)	%	Ug (m/s)	Lv (m)	%	Ug (m/s)	Lv (m)
32.12	0.162	0.125	15.96	0.134	0.074	11.73	0.122	0.036	0.52	0.063	0.0054	25.52	0.130	0.120	13.69	0.110	0.060	12.17	0.095	0.0367	0.78	0.050	0.0072	–	–	–
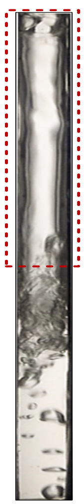												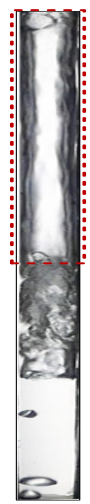			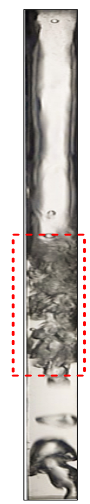			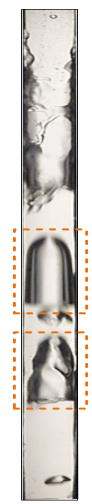						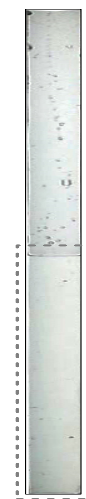		

Table 3: (B) Effects of evaporator temperature and aspect ratios on flow pattern and heat transfer when using RTPCT with the lengths of the X and Y of 25.2 mm, the aspect ratio 5, and the test angle of 90°. (When Ug is velocity of flow pattern (m/s), Lv is length of flow pattern (m)).

The evaporator temperature (°C)																				
90 °C							70 °C								50 °C					
$Q = 33.29$ W $q = 2.60$ kW/m^2							$Q = 14.29$ W $q = 1.12$ kW/m^2								$Q = 10.46$ W $q = 0.82$ kW/m^2					
Churn flow			Slug flow			Bubble flow			Churn flow			Slug flow			Bubble flow			No flow patterns		
%	Ug (m/s)	Lv (m)	%	Ug (m/s)	Lv (m)	%	Ug (m/s)	Lv (m)	%	Ug (m/s)	Lv (m)	%	Ug (m/s)	Lv (m)	%	Ug (m/s)	Lv (m)	%	Ug (m/s)	Lv (m)
17.34	0.208	0.053	7.4	0.185	0.0217	6.32	0.089	0.0051	13.21	0.198	0.041	5.17	0.180	0.0202	4.07	0.090	0.049	–	–	–

sisting of the gas and liquid flow states [23, 25, 30]. As per the evaporator temperature of 70 and 90 °C, as shown in Tab. 3(A), formation of bubble flow were accounted for 0.78% and 0.52% flow patterns respectively. Formation of slug flow were accounted for 12.17% and 11.73% of flow patterns at the same temperatures whereas churn flow were accounted for 13.69% and 15.96% repetitively. Annular flow formation were accounted for 25.52 and 32.12 at these temperatures, respectively.

Upon testing the aspect ratio 5, evaporation temperature of 50, 70, and 90 °C of RTPCT with the length of X and Y of 25.2 mm, test angle of 90°, and water as a working substance, test results as shown in Tab. 3(B), revealed that at the evaporator temperature of 50 °C, flow pattern within RTPCT was not detected. The results were similar to those of the aspect ratio of 20 as described earlier and Tab. 3(A). Upon testing with the evaporator temperature of 70 and 90 °C, three distinct flow patterns are observed, consisting of bubble flow, slug flow and churn flow. At evaporation temperature of 70 and 90 °C, accumulated heat was sufficient to vaporize the working substance. As the temperature of the evaporator also increased, the viscosity and density of the working substance in the liquid state decreased which led to vaporization of the working substance [41, 42]. Upon applying the evaporation temperature of 70 and 90 °C, as shown in Tab. 3(B), bubble flow formation were accounted for 4.07% and 6.32% of flow patterns whilst slug flow formed 5.17% and 7.40% of flow patterns, and churn flow were accounted for 13.24% and 17.34% of the flow pattern respectively. As the aspect ratio 5 has a short evaporator length, the flow distance and flow patterns change were directly affected. Therefore it was observable that, at the aspect ratio 5, three flow patterns were found including: bubble flow, slug flow, and churn flow. However, annular flow were not formed at aspect ratio 5. Flow pattern within RTPCT with the lengths of the X and Y of 25.2 mm, when tested with aspect ratio of 20, were annular and churn flow patterns. These were the main forms of the flow pattern found more often than the other types. When tested against aspect ratio 5, churn and slug flow patterns were found more frequently than other flow types.

These two-phase flow patterns float through the heat shield to transfer heat to component with lower temperature before condensing at the condensation section. After the condensation, the working substance changes its status from vapor to liquid, resulting in heavier weight of the substance, thus, adheres to the side of the pipe and move along back to the evaporator. The moving was subjected to gravity of the earth [43, 44].

4.3 Relationship of flow patterns, velocity, and heat flux

Figure 6 shows the relationship between flow patterns, velocity, and heat flux of RTPCT with the lengths of the X and Y of 25.2 mm, the aspect ratio 5 and 20, test angle of 90°, with water as working substance. The results showed that the flow pattern has changed from one flow pattern to another which directly affected the flow velocity and heat flux of each flow pattern. The heat flux has an upward trend and direction along with the change in flow pattern of each type of the flow. This, involved gradual increase of temperature of the pipe surface by heating the evaporator. Rising temperature of the pipe surface eventually surpassed the saturation temperature of the working substance. Heat transfer from the pipe wall to the working substance resulted in lower density and viscosity of the working substance. Then, the working substances reached the boiling point and began to produce bubbles and caused the fluid movement.

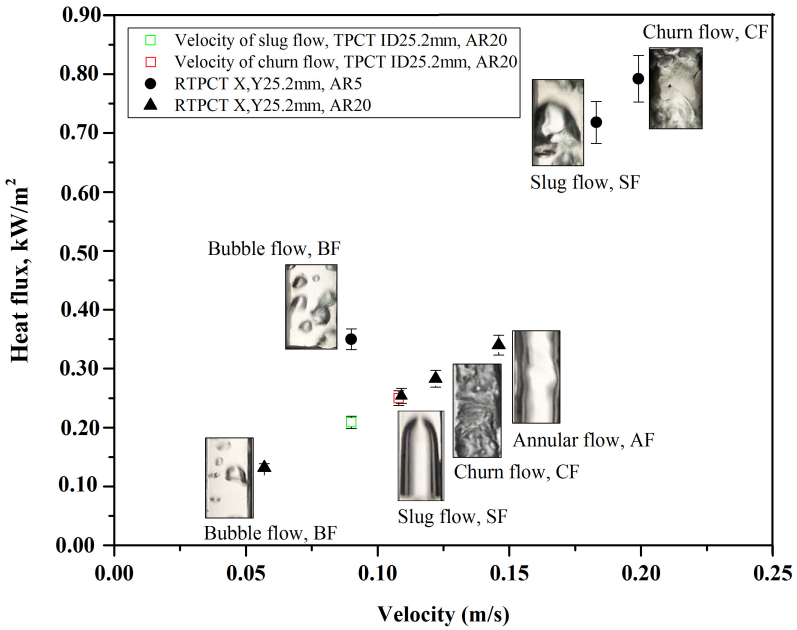

Figure 6: The relationship of flow patterns, velocity and heat flux of RTPCT with the lengths of the X and Y of 25.2 mm, the aspect ratio 5 and 20.

Flowing bubbles accumulated energy as velocity and pressure along the length of its flow. Bubble flow's increasing velocity resulted in merging of bubbles and increase in size of the bubble resembling the shape of a bullet,

thus, it is also known as the slug flow. At high speed and increased pressure, the bubble distorted and broke away causing instability. In some cases, the head of the bullet-like bubbles collided which changed the flow pattern from slug to churn flow pattern [39]. Very high bubble velocity creates hollow in the middle of the pipe where gas flows and liquid working substance film flow on the surface of the pipe. This type of flow is called annular flow [40]. When tested, aspect ratios of 20 gave rise to 4 flow patterns which were, bubble flow, slug flow, churn flow, and annular flow, respectively. For aspect ratio 5, 3 flow patterns were discovered which consisted of bubble flow, slug flow and churn flow, respectively. As aspect ratio 5 has a short evaporator length, distance of the flow pattern in the evaporator was also short as well. As a result, churn flow was not changed to annular flow, thus, three forms of flow patterns were observed. Due to short evaporator length, the moving distance from the evaporator to the condenser was relatively fast and short. Therefore, the two-phase flow patterns with the aspect ratio 5 showed a faster flow velocity and higher heat flux than those of the aspect ratio 20 as shown in Fig. 6. Upon comparing velocity and flow behaviors obtained from the tests of RTPCT with the length of the X and Y of 25.2 mm, aspect ratio of the 20 and TPCT with a diameter of 25.2 mm and aspect ratio 20 [45], results are shown in Fig. 6. According to the test results, under the same conditions, slug and churn flows that were tested by TPCT had lower flow velocity than that of the tests obtained from RTPCT. This was due to larger cross-sectional surface area of RTPCT when compared to TPCT. Furthermore, contact area was also larger in RTPCT as shown in Fig. 9. As a result, a wetted perimeter between the working substance and the inner pipe surface of the RTPCT was greater than that of TPCT. Therefore, when the evaporator of the RTPCT was heated, its working substance was heated quicker and the following flow patterns were continuous and consistent. This also including a vigorous boiling of the work substances as shown in Fig. 7.

RTPCT was built with equal structure and sizes of all three parts – evaporator section, adiabatic section, and condenser section, thus, bubble flow was able to combine and change to other flow pattern rather quickly. Thus, thickness of the liquid film created by the condensation was distributed evenly and throughout the area of the condenser. Such liquid film in the condensation is thin and helps to reduce friction of the movements from the two-phase flow [9]. Therefore, slug and churn flows of RTPCT were moving at higher velocity than the same flow patterns that occurred within the TPCT, as shown in Fig. 6.

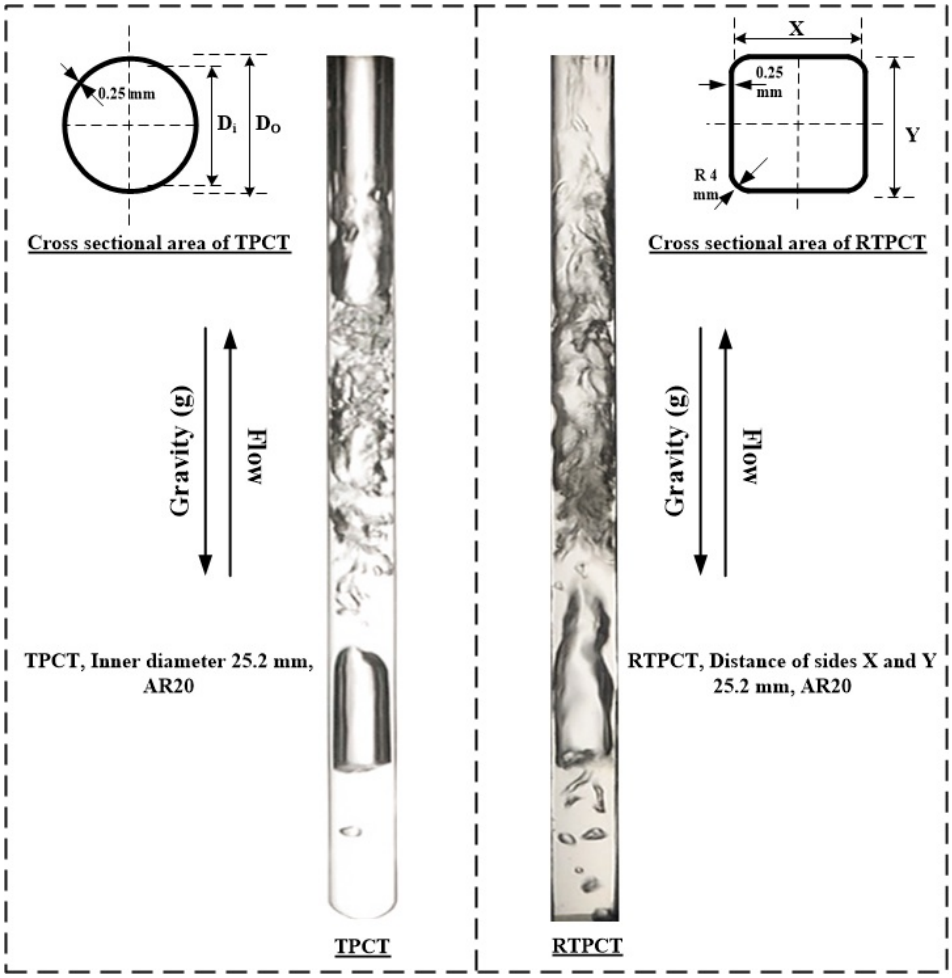

Figure 7: Behavior comparisons between RTPCT with the length of the X and Y of 25.2 mm and TPCT with a diameter of 25.2 mm at the aspect ratio of 20.

4.4 Effects of evaporator temperature and aspect ratio that influence the heat flux

Figure 8 shows a relationship between the evaporator temperature and the aspect ratio that affect the heat flux of RTPCT with the length of X and Y of 25.2 mm, aspect ratio 5 and 20. The figure also shows that when the evaporator temperature rises, the heat flux or heat transfer per unit area also becomes higher. This is due to specific heat capacity of the working

substance that increases in accordance with the evaporator's temperature, including a higher heat transfer coefficient that occurred within the RTPCT. As per the result, RTPCT with a length of X and Y of 25.2 mm, aspect ratio of 5, and the average heat flux that were higher than all other test cases. Average heat flux throughout the test was 1.51 kW/m^2. The aspect ratio 20 provided the average heat flux of 0.74 kW/m^2, which in generally, the aspect ratio of ($L_e/4R_h$, L_e/D_i) is regulated by evaporator length. Therefore, the changing aspect ratio also affected the evaporation length of RTPCT as well. Furthermore, addition ratio of the working substance also changed according to the volume ratio of the evaporator. The aspect ratio 5 has a short evaporator length which can be calculated from the equation of the aspect ratio as shown in Fig. 8. Thus, this was another reason that caused the vapor bubbles to briefly and rapidly ascended to the condenser to release the heat before flowing to the evaporator to absorb the heat again.

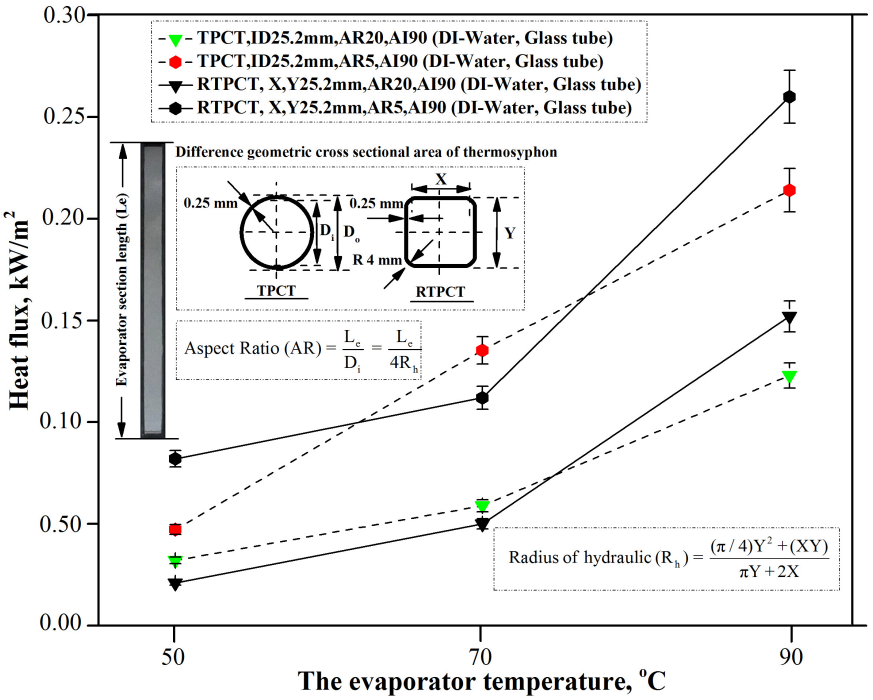

Figure 8: The relationship between evaporation temperature and the aspect ratio that affects the heat flux of RTPCT with X and Y lengths of 25.2 mm, and aspect ratio of 5 and 20.

The heat flux as obtained from the test of RTPCT with the lengths of X and Y of 25.2 mm and the aspect ratio 5 and 20, compared with that of TPCT with a diameter of 25.2 mm and the aspect ratio 5 and 20 [45] can be illustrated as per Fig. 8. According to the results, average heat flux throughout the test obtained from RTPCT was higher than the average heat flux obtained from every test using TPCT under the same test conditions. This was due to the nature of the contact area of RTPCT as shown in Fig. 9. This partially helped to eliminate heat resistance between the

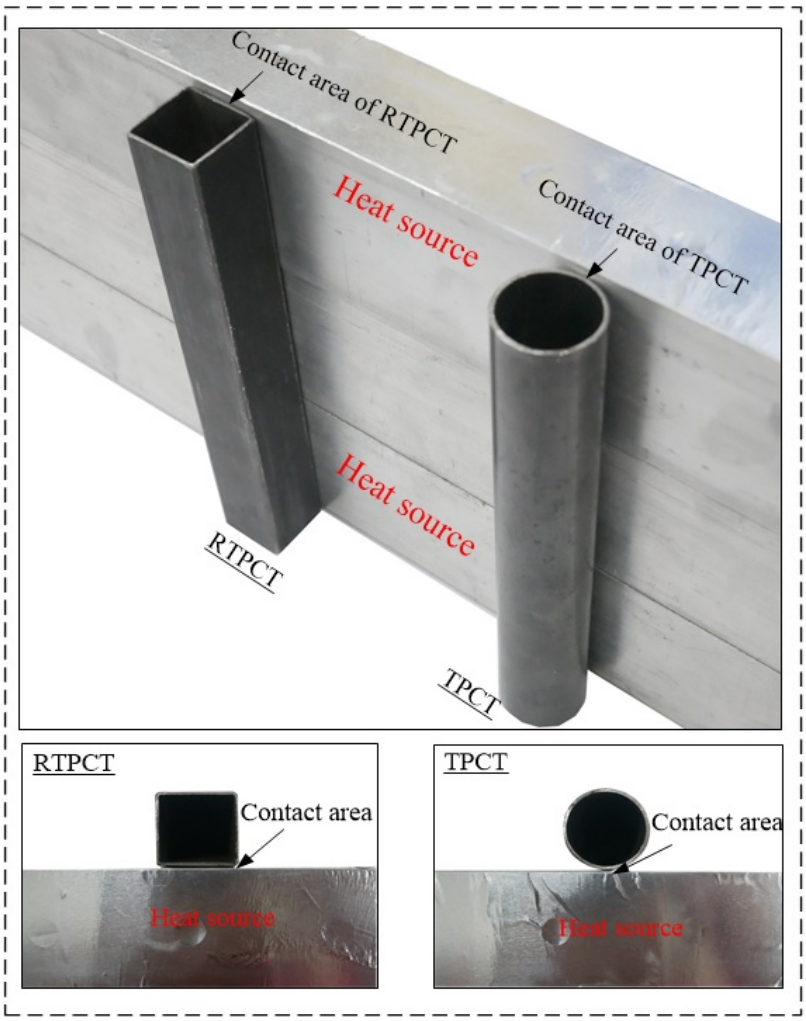

Figure 9: The surface area of RTPCT and TPCT [7].

heat source and the external surface of the evaporator, and heat resistance between external surface of the condenser and heat releaser Z_1 and Z_9 respectively. From the test found that The average heat flux throughout the test received from RTPCT is higher than the heat flux. As a result, the total heat resistance of RTPCT was lower than that of TPCT, which helped to improve the boiling of the working substance [7] as shown in Fig. 3. This also resulted in higher average heat flux throughout the test, as obtained from RTPCT, when compared to the average heat flux obtained from the test with TPCT under the same test conditions as shown in Fig. 8.

5 Summary

Testing of RTPCT with aspect ratio 5, test angle of 90°, using water as working substance at evaporation temperatures of 70 and 90 °C produced 3 flow patterns; bubble flow, slug flow, and churn flow respectively. Slug flow and churn flow are the main flow patterns that can affect the heat flux.

Testing of RTPCT with the aspect ratio 20, test angle of 90°, using water as working substance, at evaporation temperatures of 70 and 90 °C revealed four flow patterns consisting of bubble flow, slug flow, churn flow, and annular flow respectively. Churn flow and annular flow are the main types of flow that can affect the heat flux.

Upon comparing behavioral differences and flow patterns that were altered by aspect ratios and evaporating temperatures, where water was used as working substance, such altered aspect ratios and evaporating temperatures were found to have direct effects on the occurrence and behavior of the two-phase flow patterns. Bubble flow, slug flow, and churn flow were the basic flow patterns associated with the test with aspect ratio 5 and 20, respectively. Annular flow was only found when tested with the aspect ratio of 20 and different evaporator length that were regulated by the difference of such aspect ratios. Therefore, the aspect ratio 20 was determined to have sufficient length of the evaporator that can transform the flow pattern from churn flow to annular flow.

Rising evaporator temperature resulted in higher heat flux or heat transfer per unit area. The highest heat flux was found at the evaporator temperature of 90 °C when tested with RTPCT at the aspect ratio 5 and 20. The highest obtained heat fluxes were 2.60 and 1.52 kW/m^2 for 5 and 20 aspect ratio respectively.

Changes of geometric cross-sectional surface area of the TPCT is controlled by an inner diameter of 25.2 mm when changed to the wetted perimeter. This is the controlled characteristic of the RTPCT with the length of the X and Y of 25.2 mm. The RTPCT's rectangular cross-section surface area provides greater contact area, when compared to TPCT, to receive and release the heat. This also helps to eliminates heat resistance between the heat source and the external surface of the evaporator (Z_1) as well as eliminating heat resistance between the external surface of the condenser and the heat releaser (Z_9), respectively. Therefore, RTPCT has less total heat resistance (Z_{total}) than TPCT. In addition, RTPCT permits the liquid film from the condenser to distribute its thickness evenly and throughout. As RTPCT's condensation area is greater than that of the TPCT, thinner liquid film in the condenser section can be formed.

Acknowledgments This research work was conducted at the Heat Pipe and Thermal Tool Design Research Unit (HTDR), Faculty of Engineering, Mahasarakham University, Mahasarakham, Thailand.

Received in February 2019

References

[1] Al-Waeli A.H.A., Chaichan M.T., Sopian K., Kazem H.A.: *Influence of the base fluid on the thermo-physical properties of PV/T nanofluids with surfactant.* Case Stud. Therm. Eng. **13**(2019), 100340.

[2] Reay D., Kew P.: *Heat pipe, Theory, Design and Application.* 5th Edn. Butterworth-Heinemann, 2006.

[3] Noie S.H., Sarmasti Emami M.R., Khoshnoodi M.: *Effect of inclination angle and filling ratio on thermal performance of a two-phase closed thermosyphon under normal operating conditions.* Heat Transfer Eng. **28**(2007), 4, 365–371.

[4] Terdtoon P., Chailungkar M., Shiraishi M.: *Effects of aspect ratios on internal flow patterns of an inclined closed two-phase thermosyphon at normal operating condition.* Heat Transfer Eng. **19**(1998), 4, doi.org/10.1080/01457639808939938.

[5] Teoh C.K., Maschmann M.R., Ma H.B.: *Heat-transfer analysis in heat sink embedded with a thermosyphon.* J. Thermophys. Heat Tr. **17**(2003), 3, 348–353.

[6] Shafahi M., Bianco V., Vafai K., Manca O.: *An investigation of the thermal performance of cylindrical heat pipes using nanofluids.* Int. J. Heat Mass Tran. **53**(2010), 1–3, 376–383.

[7] Bhuwakietkumjohn N., Parametthanuwat T.: *Heat transfer behaviour of silver particles containing oleic acid surfactant: application in a two phase closed rectangular cross sectional thermosyphon (RTPTC).* Heat Mass Transfer **53**(2016), 1, 37–48.

[8] Parametthanuwat T., Bhuwakietkunjohn N.: *I-shape-two phase closed thermosyphon: A thermal behaviour study.* In: Proc. 5th Int. Conf. on Science, Technology and Innovation for Sustainable Well-Being (STISWB V), Luang Prabang, Lao PDR, 2013, 45.

[9] Srimuang W., Rittidech S., Bubphachot: *Heat transfer characteristics of a vertical flat thermosyphon (VFT).* J. Mech. Sci. Technol. **23**(2009), 9, 2548–2554.

[10] Srimuang W.: *Factors affecting the heat transfer characteristics of different geometric cross sectional area thermosyphon (DGCST).* Dissertation, Mahasarakham Uni., 2010.

[11] Amatachaya P., Srimuang W.: *Comparative heat transfer characteristics of a flat two-phase closed thermosyphon (FTPCT) and a conventional two-phase closed thermosyphon (CTPCT).* Int. Commun. Heat Mass **37**(2010), 3, 293–298.

[12] Moon G.H.S.H., Yun H.G., Choy T.G., Kang Y.I.: *Improving thermal performance of miniature heat pipe for notebook PC cooling.* Microelecton. Reliab. **42**(2002), 1, 135–140.

[13] Moon G.H.S.H., Ko C., Kim Y.T.: *Experimental study on the performance of micro-heat pipe with cross-section of polygon.* Microelectron. Reliab. **44**(2004), 2, 315–321.

[14] Hussein H.M.S., Ghetany H.H.-El., Nada S.A.: *Performance of wickless heat pipe flat plate solar collectors having different pipe cross sections geometries and filling ratios.* Energy Convers. Manage. **47**(2006), 11–12, 1539–1549.

[15] Zhang M., Liu Z., Ma G.: *The experimental investigation on thermal performance of a flat two-phase thermosyphons.* Int. J. Therm. Sci. **47**(2008), 9, 1195–1203.

[16] Khazaee I., Hosseini R., Noie S.H.: *Experimental investigation of effective parameters and correlation of geyser boiling in a two-phase closed thermosyphon.* Appl. Therm. Eng. **30**(2010), 5, 406–412.

[17] Tadrist L.: *Review on two-phase flow instabilities in narrow spaces.* Int. J. Heat Fluid Fl. **28**(2007), 1, 54–62.

[18] Khodabandeh R., Furberg R.: *Instability, heat transfer and flow regime in a two-phase flow thermosyphon loop at different diameter evaporator channel.* Appl. Therm. Eng. **30**(2010), 10, 1107–1114.

[19] Paramatthanuwat T., Boothaisong S., Rittidech S., Booddachan K.: *Heat transfer characteristics of a two-phase closed thermosyphon using de ionized water mixed with silver nano.* Heat Mass Transfer **46**(2010), 3, 281–285.

[20] Smith K., Kempers R., Robinson A.: *Confinement and vapour production rate influences in closed two-phase reflux thermosyphons Part A: flow regimes.* Int. J. Heat Mass Tran. **119**(2018), 907–921.

[21] Grooten M., Van der Geld C., Van Deurzen L.: *A study of flow patterns in a thermosyphon for compact heat exchanger applications.* In: Proc. 5th Int. Conf. on Transport Phenomena in Multiphase Systems, HEAT **2**(2008), 323–328.

[22] Asirvatham L.G., Wongwises S., Babu J.: *Heat transfer performance of a glass thermosyphon using graphene–acetone nanofluid.* J. Heat Transf. **137**(2015), 11, 111502.

[23] Shiraishi M., Terdtoon P., Murakami M.: *Visual study on flow behavior in an inclined two-phase closed thermosyphon.* Heat Transfer Eng. **16**(1995), 1, 53–59.

[24] Su H., Li T., Jiang Y., Guo C., Wang T.: *Experimental study on visualization of U-shaped array thermosyphon.* Appl. Therm. Eng. **152**(2019), 917–924.

[25] Bhuwakietkumjohn N., Rittidech S.: *Internal flow patterns on heat transfer characteristics of a closed-loop oscillating heat-pipe with check valves using ethanol and a silver nano-ethanol mixture.* Exp. Therm. Fluid Sci. **34**(2010), 8, 1000–1007.

[26] Agunlejika E.O., Langston P., Azzopardi B.J., Hewakandamby B.N.: *Flow instabilities in a horizontal thermosyphon reboiler loop.* Exp. Therm. Fluid Sci. **78**(2016), 90–99.

[27] Pabón N.Y.L., Mera J.P.F., Vieira G.S.C., Mantelli M.B.H.: *Visualization and experimental analysis of Geyser boiling phenomena in two-phase thermosyphons.* Int. J. Heat Mass Tran. **141**(2019), 876–890.

[28] Wei L., Yuan D., Feng Y., Tang D.: *Experimental study of bubble growth and Flow in small-diameter thermosyphon loops with filling ratios of 90% and 95%.* J. Enhanc. Heat Transf. **21**(2014), 1.

[29] Charoensawan P., Terdtoon P.: *Visual study on two-phase flow in a horizontal closed-loop oscillating heat pipe.* Therm. Sci. **23**(2019), 2B, 1055–1065.

[30] Huo X., Chen L., Tian Y., Karayiannis T.: *Flow boiling and flow regimes in small diameter tubes.* Appl. Therm. Eng. **24**(2004), 8-9, 1225–1239.

[31] Xia G., Wang W., Cheng L., Ma D.: *Visualization study on the instabilities of phase-change heat transfer in a flat two-phase closed thermosyphon.* Appl. Therm. Eng. **116**(2017), 392–405.

[32] Srimuang W., Amatachaya P., Krittacom B.: *Thermal performance of a flat two phase closed thermosyphon (FTPCT) with different cross-sectional areas and source temperatures.* In: Proc. 10th Int. Heat Pipe Symp. Tamsui, New Taipei City, Taiwan, 2011, 147–152.

[33] Anon: *Heat pipes-general information on their use, operation and design.* Data Item No. 80013. Engineering Sciences Data Unit, London 1980.

[34] Frank P., Incropera D., Dewitt P.: *Fundamental of Heat and Mass Transfer* 4th Edn. Wiley, New York 1996.

[35] Bell S.A.: *A Beginner's Guide to Uncertainty of Measurement.* Measurement Good Practice. Guide No. 11, NPL, Middlesex, 2001.

[36] Pipatpaiboon N., Rittidech S., Meena P.: *Experimental study of a thermosyphon heat exchanger (TPHE) in a bio-diesel factory in Thailand.* Arab. J. Sci. Eng. **37**(2012), 7, 2047–2060.

[37] Locke G. (Ed.): T*he Tubular Thermosyphon: Variations on a Theme.* : Oxford Univ. Press, New York 1992.

[38] Tamaki S. *et al.*: *Effects of an internal heat exchanger in a refrigerant system with carbon dioxide on its cooling coefficient of performance and cooling capacity.* Kagaku Kogaku Ronbun. **34**(2008), 5, 505–512.

[39] Liu S., Li J., Chen Q.: *Visualization of flow pattern in thermosyphon by ECT.* In: Proc. AIP Conf. Proc. **914**(2007), 1, 775–785.

[40] Terdtoon P.: *Boiling*. Chiang Mai Uni., 2001.

[41] Lamaison N., Marcinichen J.B., Szczukiewicz S., Thome J.R., Beucher: *Passive two-phase thermosyphon loop cooling system for high-heat-flux servers*. Interfac. Phenom. Heat Transf. **3**(2015), 4, 369–391.

[42] Khandekar S., Joshi Y.M., Mehta B.: *Thermal performance of closed two-phase thermosyphon using nanofluids*. Int. J. Therm. Sci. **47**(2008), 6, 659–667.

[43] Franco A., Filippeschi S.: *Closed loop two-phase thermosyphon of small dimensions: A review of the experimental results*. Microgravity Sci. Tec. **24**(2012), 3, 165–179.

[44] Smith K., Siedel S., Robinson A.J., Kempers: *The effects of bend angle and fill ratio on the performance of a naturally aspirated thermosyphon*. Appl. Therm. Eng. **101**(2016), 455–467.

[45] Sichamnan S.: *Flow Patterns and Heat Transfer Characteristic of Two-Phase Closed Rectangular Cross Sectional Area Thermosyphon*. Dissertation, Mahasarakham Uni., 2019.